

# Numerical Simulation of the Angle of Groyne Installation on the Separation Zone Length Behind it

Hamid Shamloo<sup>1</sup> and Bahareh Pirzadeh<sup>2,\*</sup>

<sup>1</sup> Associate Professor at K.N. Toosi University of Technology

<sup>2</sup> Assistant Professor at University of Sistan and Baluchestan

## ABSTRACT

Groynes are usually installed along the river side and those are used for a lot of application such as bank protection. These structures would be changed the flow pattern and prevent bank erosion. So understanding turbulent flow pattern around groynes for designing groyne installation criteria is very important. In this paper subcritical flow pattern around an indirect groyne in six different angle of installation was established and 3D simulations in Fluent software have been applied to investigate the effect of angle of groyne installation on separation zone length behind it. In all cases the groyne length and inlet flow depth were constant and the bed slope of the channel was zero. Good agreements were found between numerical and experimental results. Results showed that the separation length is about 12 times the impermeable groyne with 0.3m length. Also, the incidence angle was about 5 degree that was in a very good consistence with the referred experimental data.

## KEYWORD

Groyne, angle of installation, separation, Fluent, Parallel processing

## INTRODUCTION

Groynes are structures that are aimed at diverting the flow from the river embankment. These structures create an appropriate path for guiding the flow and limiting the movements of sediments. Accurate estimates of the physical processes that lead to the erosion of the river sides are very important because erosion can cause significant economic and environmental problems such as land loss, risk exposure and damage to aquatic location and hydraulic structures. If erosion doesn't control, it can be considered as a source of sediment load. For example, about 60 percent of the sediment in the river is directly related to the sediment

Derived from the erosion of the river side [1]. Because of the wide applications of these structures in river and coastal engineering, in addition to the numerical and experimental studies in the past, many researches have been conducted in recent years, such as experiments by Ettema, R., Muste, M. (2004) [2]. They presented the flow-thalweg alignment around a dike, and area extent of the wake immediately downstream of a dike. The experiments show that use of a shear-stress parameter as the primary criterion for dynamic similitude influences these features [2]. In 2005, Uijtewaal studied the flow pattern around the groynes with different shapes experimentally [3]. He aimed at finding efficient alternative designs (various groin shapes), in the physical, economical, and ecological sense, for the standard groins in the large rivers of Europe. According to their observation, it was demonstrated that the turbulence properties around the groyne can be manipulated by changing the permeability and slope of the groin head. It was also shown that for submerged conditions the flow becomes more complex and locally dominated by three-dimensional effects [3]. In the same year, three dimensional numerical study of flow around groynes was conducted by Nagata et al. [4]. They used non-linear k-ε turbulence model and calculated the temporal change in bed topography by coupling a stochastic model for sediment pickup and deposition using a momentum equation of sediment particles to evaluate the capability of the developed model [4]. Also, Yeo et al. performed some experiments (69 experiments) to produce a design guideline in Korea and to examine the downstream separation region of a groyne under various groyne lengths and installation angles with various degrees of groyne permeability [5]. In 2006, Karami's experiments aimed at evaluating the effects of a side dike on the scour pattern around the dike nose [6]. In the same year, a similar study using Large Eddy Simulation technique for three-dimensional simulations of the flows around a non-submerged spur dike, performed by Xuelin et al. to analyse the vortex flows around the spur dike. They also conducted an experiment in a wide flume with a dike placed as a barrier to compare with their numerical results [7]. Yossef

\*Corresponding Author: Bahareh Pirzadeh

E-mail : b\_pirzadeh@eng.usb.ac.ir

Telephone Number :

Fax. Number :

and Ruppercht concurrent laboratory study aimed to investigate the morphological interaction between the groyne fields and main channel. They compared their experimental study with their numerical results using DELFT3D and found that this code is qualitatively well in computing the morphological pattern [8]. In 2007, Ghodsian et al. Examined the effect of groyne position in a 90 degree bend on the size of the separation zone behind it. They performed several experiments by changing the groyne length (three different lengths) and its position (5 different positions) and investigated the characteristics of the separation zone behind the groyne [9]. In the same year, flow pattern around a groyne predicted by  $k-\epsilon$  turbulence model in two dimensional Fluent software by Keshavarz et al. [10]. They found that the separation length is smaller for inclined groynes compared with the perpendicular ones [10]. Ho et al. in 2007 built some simulations (four different ratios of groyne length to channel width and five different porous groynes) in Flow3D software to simulate the groyne tip velocity and the flow separation length near the groyne [11]. They proposed a relationship of the ratio of the separation length to groyne length with Froud number [11]. Minor et al. compared a numerical model with measured laboratory data to examine the turbulent flow and associated sediment transport due to a series of submerged groynes in a channel bend [12]. Their statistical comparison of the equilibrium bed geometry found average regression coefficients of determination of 0.77 and 0.72 for the 90° and 135° channels, respectively [12]. Teraguchi et al. compared permeable and impermeable groynes in terms of river bed changes through hydraulic model experiments and simulation numerical tests [13]. Their finding showed that the local scour hole around the upstream groyne is deeper in the case of impermeable groynes than permeable ones [13]. Experimental study on the flow characteristics around the refraction groyne performed by Kang et al. in 2011 to investigate the flow influences around the groyne due to changes in the arm angle and length [14]. Their results showed that velocity increase in main channel is greater for the upward groynes than downward ones. Also, the vortices at recirculation area of these groynes, had different shapes. It was found that the length of the recirculation area, was 10.2-14.7 times for upward groynes, 8.4-12.7 times for downward groynes, and 10.6-13.8 times for right angle groynes, the projection length incensement [14]. Three-dimensional flow around a groyne was simulated in Flow-3D software using large-eddy turbulence model by Shahrokhi and Sarveram in 2011 [15]. They studied the effects of groyne structure on separation length and width of separation region behind it [15]. Their results showed that the maximum separation length and width were related to installation angle on 105 degree [15]. Flow past a spur dyke on a rigid bed meandering channel with a trapezoidal cross section studied experimentally by Sharma and Mohapatra in 2012 [16]. Their results showed that the length of the downstream separation zone varies from 4 to 22.8 times the spur dike length [16].

Improvements in software functionality and increasing the speed and accuracy compared to laboratory studies in one

hand and the lack of three dimensional simulations to explore the effects of groyne installation angle on the velocity on its nose and dimension of the separation zones around the groyne, in the other hand, encouraged us to perform a numerical study of the flow pattern around a groyne and examine the groyne construction angle towards the approaching flow on the length of downstream separation zone formed due to the presence of the groyne. For this purpose, the experiments of Yeo et al. have been selected to compare the obtained numerical results from this research. The separation zone length, velocity value on the groyne nose, and incidence angle have been compared to Yeo et al. experimental data [5] that showed a good agreement.

### FLOW PATTERN AROUND THE GROUYNE

Groynes are classified in different groups based on their infiltration rate, submergence ratio, and the groyne installation angle [17] shown in Fig.1. A permeable groyne allows water to flow through the reduced velocity, compared to the impermeable ones that block and deflect the flow. A deflecting groyne shifts deep scour away from the river side, an attracting groyne creates deep scour near the bank, and a repelling groyne force the flow away from themselves. Finally, depending on the degree of flow disturbance needed, groyne can be submerged or not [17].

The flow area around a groyne can be divided into three regions (Fig.2) [18]. The main flow area where flow is disturbed by the groyne within the watercourse covers the area from the groyne nose toward the river side, the recirculation area formed in the downstream part of the groyne, and the mixing zone between these two regions. The wake zone may possibly divide into the return flow region and the reattachment zone. The return flow is generally characterized by two different rotation direction of eddy size and specific. The smaller eddy is in the vicinity of the groyne and its centre is located at a distance approximately equal to the length of the groyne. The bigger eddy is placed downstream of the smaller eddy and its centre is located at a distance of about six times the groyne length. The reconnection region is the area where the separated flow reattaches the riverside in the downstream of the groyne [18]. The length of this region covers about six times the length of groyne and is placed in the range of 11-17 times the length of the groyne [19]. The main feature of the mixing region is that it is a zone in where vortexes stretch and periodic fluctuations in water level are clear [18].

### GEOMETRICAL SETUP OF SIMULATED CASES

Numerical results obtained from the current study have been compared with the reported experimental data of Yeo et al. Their experimental set-up was 40 m long open channel flume with a rectangular cross-section with 2 m in width and 0.65 m in depth [5]. The approaching flow was well-developed and the channel slope and bed roughness were considered zero [5]. The groyne length (l) was 30cm. A

schematic sketch of the flume in X-Y plane is shown in Fig.3.

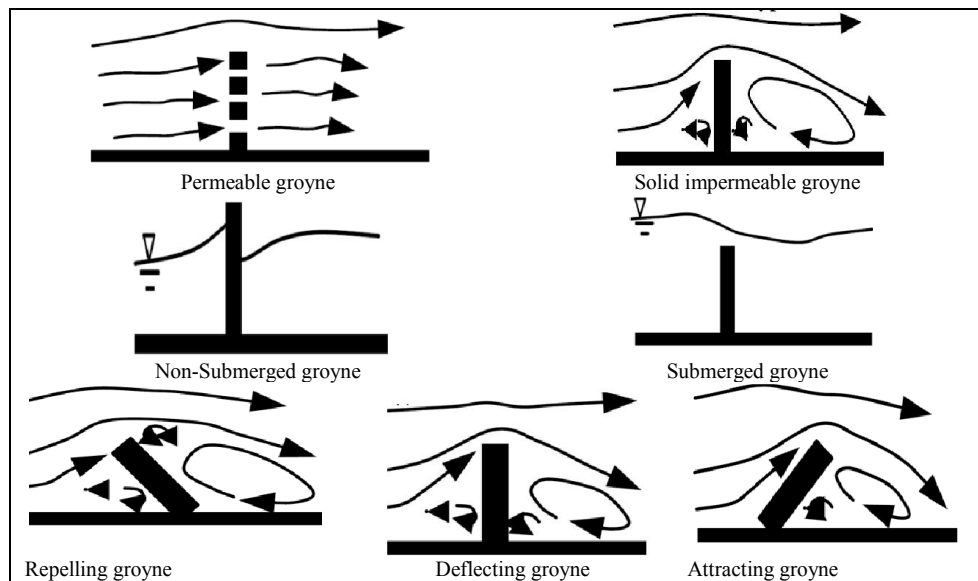


Fig1. Groyne classification according to the material of construction, groyne height below high water, and to the function it serves [17].

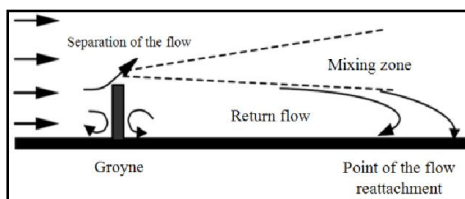


Fig2. Flow zones around a single groyne [18]

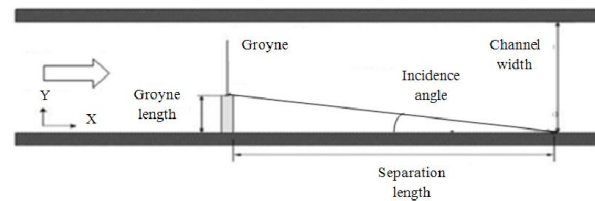


Fig3. Schematic sketch of the simulated flume in horizontal plane [5]

## NUMERICAL MODEL DESCRIPTION

FLUENT is the CFD solver for complex flow ranging from incompressible to highly compressible flows. It provides multiple choices of solver option, combined with a convergence-enhancing multi-grid method. Because of its optimum solution efficiency and accuracy, it has been selected to simulate the groyne in this research.

The FLUENT's parallel solver has the ability to use multiple processors that may be executing on the same computer, or on different computers in a network to decrease the computing time [20]. This capability has been used in the present study using a dual core computer in order to reduce the simulation time and numerical efforts.

Conservative form of the Navier-Stokes equations using the Finite Volume method on structured Cartesian coordinate grid system applied to solve the flow parameters. Reynolds Stress turbulence model (RSM) in Fluent software, applied to estimate the turbulent flow field. The details of governing equations and RSM model can be found in FLUENT user's guide [20].

In all cases simulated in this study, a fully one-order implicit scheme was applied for temporal discretization and a second order central differencing scheme for space discretization. Also, the SIMPLE method was adopted for the velocity-pressure coupling on the form of steady state solution. Also, the RSM turbulence model has been carried out for simulating the turbulent flow around the groyne.

## MESH RESOLUTION AND BOUNDARY CONDITIONS

Appropriate condition must be specified at domain boundaries depending on the nature of the flow. In the simulation performed in this study, an inlet for water with a velocity inlet boundary condition was specified and the uniform velocity magnitude was set to the mean velocity. Outflow and symmetry boundary conditions at outlet and at the top surface were used, respectively. The no-slip boundary condition is specified to set the velocity to be zero at the solid boundaries and walls.

It is also important to establish a grid structure to be fine enough especially near the wall boundaries and the groyne,

which is the region of rapid variation. The location of the first grid point near the wall was set 0.001m and the mesh stretched out in the wall-normal direction. A total of about 600000 computational nodes were used for each case.

## RESULTS

In this paper, three dimensional numerical investigations have been performed for evolution of the ability of an available 3D commercial flow solver to cope with the fully turbulent flow around a groyne. Six different angles of installations were examined to investigate its effect on flow pattern in an open channel. The details are presented as following.

According to the performed investigations, the presence of groyne affects the turbulent flow field. The comparison of the referred experimental data and obtained numerical results from this study confirms the accuracy of the performed numerical simulations to estimate the separation zone length downstream of the groyne, which is mentioned in table 1. Understanding this length can provide helpful advice for the groyne installation interval. Figs. 4 to 9 demonstrate the stream-wise velocity contour downstream of the groyne for the simulated cases.

According to these figures, the presence of the curvature of the flow is clear. As it is expected, by acting the flow around the groyne, this structure tends to enhance local velocities in their vicinity. The results indicate that with an increase in groyne installation angle, the difference between velocity values in the main flow region and the return flow area increases. This phenomenon shifts the location of the return flow centre away from the channel side-wall.

Table 2 represent the numerical values of velocities on the groyne nose and the incidence angle compared to the experimental data of Yeo et al. According to the results, a satisfying agreement has been obtained for velocity values. Also, the accuracy of the obtained results for incidence angle is well. This angle is obtained about 5 degree which is in consistence with the experimental data of Yeu et al who also presented a formula based on the groyne length to the channel width ratio (Eq 1). Using this equation, the incidence angle for a groyne with 30cm length is obtained 4.78 degree that is very close to our numerical results shown in table 2.

$$\text{Incidence angle} = -1.662 (\text{groyne length} / \text{channel width}) + 5.031 \quad (1)$$

Tab1. Comparison of the separation length downstream of a groyne

No.	Angle of groyne installation	Inlet velocity (m/s)	Froud number	Separation length (m)		Error percentage	$L_{exp}/l$	$L_{num}/l$
				Yeo et al. experiments ( $L_{exp}$ )	Obtained results ( $L_{num}$ )			
1	120	0.23	0.19	3.50	3.46	1.14	11.67	11.53
2	105	0.23	0.19	3.80	3.87	1.84	12.67	12.90
3	90	0.25	0.21	3.60	3.53	1.94	12.00	11.77
4	75	0.25	0.21	3.65	3.64	0.27	12.17	12.13
5	60	0.25	0.21	3.40	3.31	2.65	11.33	11.03
6	45	0.25	0.21	2.90	2.92	0.69	9.67	9.73

Tab2. Comparison of the velocities on the groyne nose and the incidence angle

No.	Angle of groyne installation	Velocity on the groyne nose (m/s)		Error percentage for velocity	Incidence angle	
		Exp.	Num.		Exp.	Num.
1	120	0.29	0.28	3.45	5.91	4.12
2	105	0.32	0.301	5.94	5.04	4.20
3	90	0.35	0.337	3.71	4.70	4.86
4	75	0.33	0.328	0.61	4.76	4.66
5	60	0.32	0.289	9.69	4.51	4.70
6	45	0.30	0.273	9.00	4.90	4.48

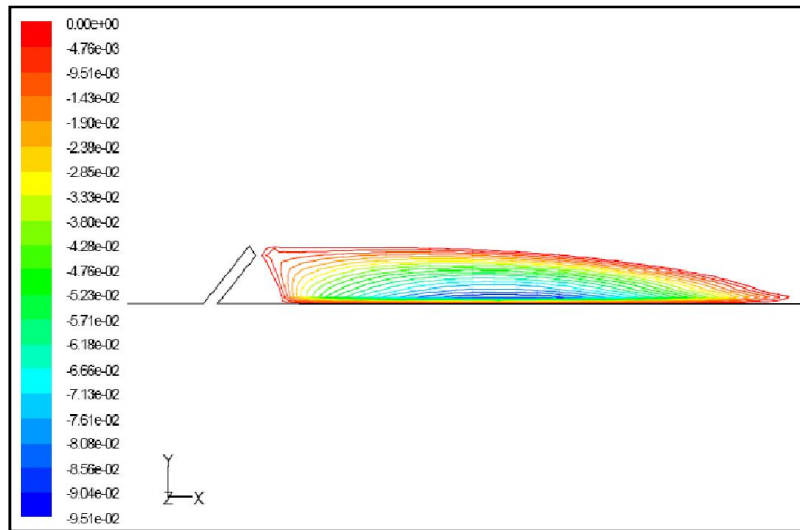


Fig. 4 .Stream-wise velocity contours downstream of a groyne with installation angle of 45°

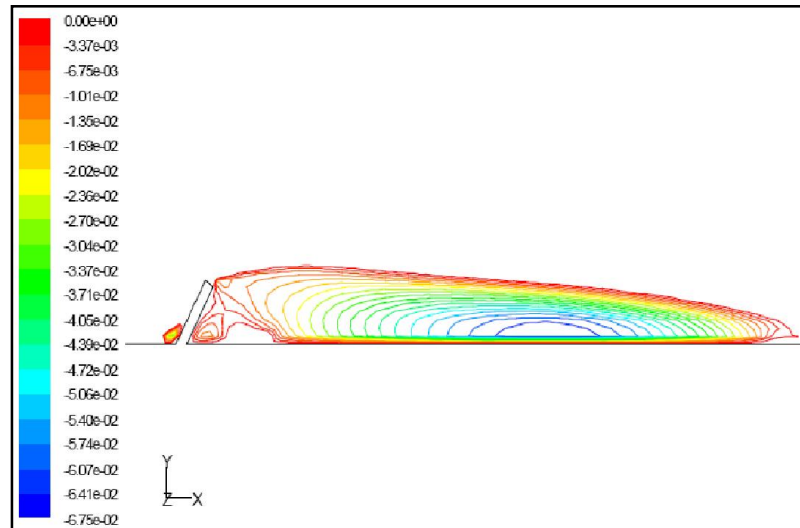


Fig. 5 .Stream-wise velocity contours downstream of a groyne with installation angle of 60°

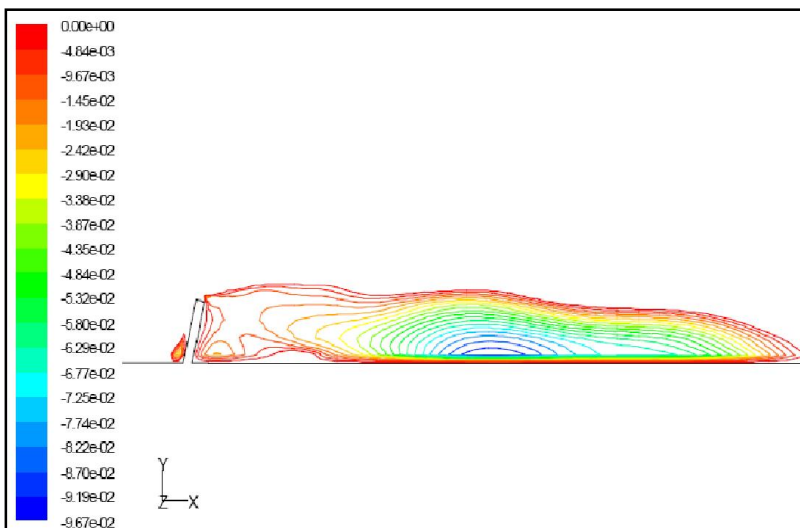


Fig. 6 .Stream-wise velocity contours downstream of a groyne with installation angle of 75°

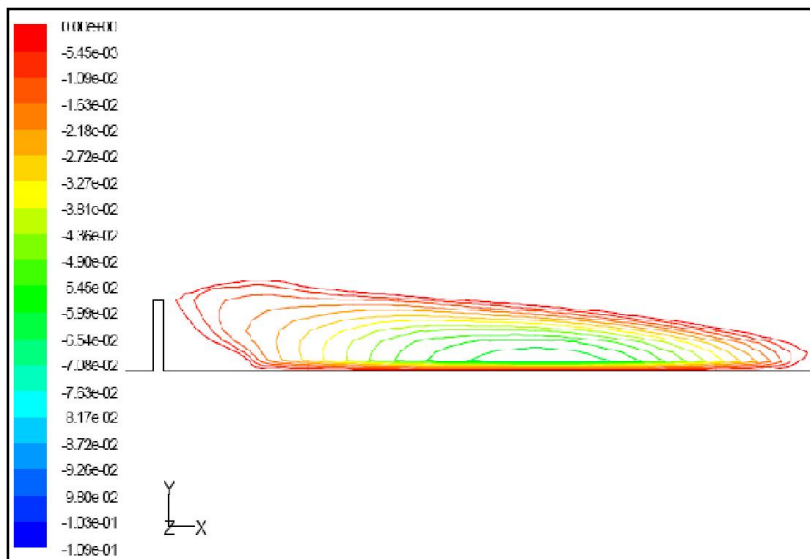


Fig. 7 .Stream-wise velocity contours downstream of a groyne with installation angle of 90°

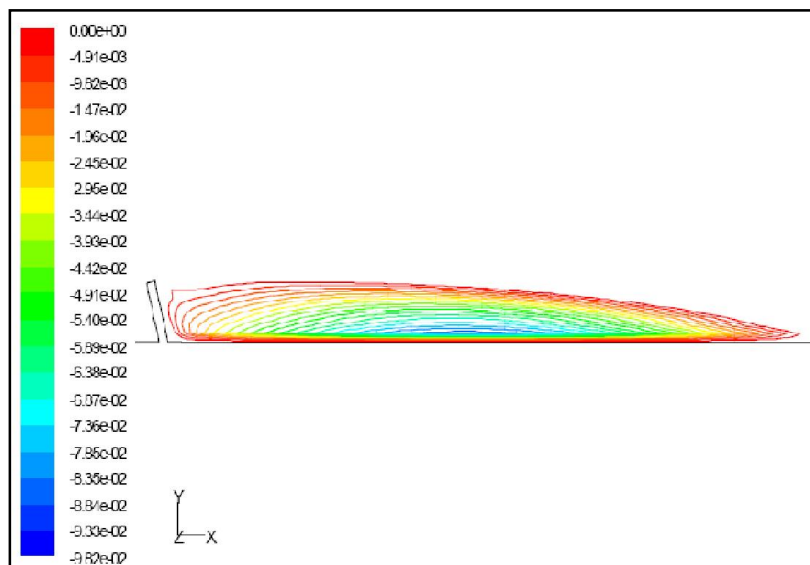


Fig. 8 .Stream-wise velocity contours downstream of a groyne with installation angle of 105°

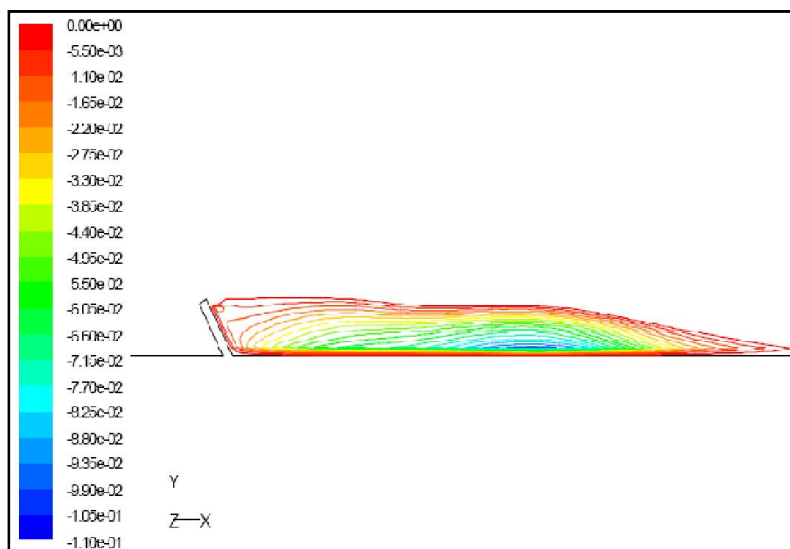


Fig. 9 .Stream-wise velocity contours downstream of a groyne with installation angle of 120°

## CONCLUSION

Because a groyne serves to maintain a desirable channel for the purpose of flood and erosion control improved navigation, in this study flow pattern changes induced by a single groyne in a rectangular open channel were numerically simulated using a three-dimensional Finite Volume CFD model to investigate the effect of groyne installation angle. The numerical model was simulated with various groyne installation angles. Comparison of the velocity value on the groyne nose, the separation length downstream of the groyne, and the incidence angles with the physical model measurements completed by Yeo et al. (2005) showed a very satisfying agreement. The separation length provided good knowledge of the groyne installation interval. It showed that, it is about 12 times the impermeable groyne with 0.3m length. Results also declared that with an increase in groyne installation angle, the location of the return flow area centre shifts away from the channel side-wall. The incidence angle was about 5 degree that was in a very good consistence with the referred experimental data.

## REFERENCES

- [1] **Ercan A. & B. A. Younis.** Prediction of Bank Erosion in a Reach of the Sacramento River and its Mitigation with Groyne, *Water Resour Manage.* Vol23, Issue 15, 2009, pp. 3121-3147.
- [2] **Ettema , R., Muste, M.** Scale Effects in Flume Experiments on Flow around a Spur Dike in Flatbed channel, *Journal of Hydraulic Eng.,* Vol. 130, 2004, pp. 635-646.
- [3] **Uijtewaal, W.S.J.** Effect of groin layout on the flow in groin field: laboratory experimental, *Journal Hydraulic Eng., ASCE,* Vol. 131, No.9, 2005, pp.782-791.
- [4] **Nagata, N., Hosoda, T., Nakato, T. and Muramoto, Y.** Three-dimensional numerical model for flow and bed deformation around river hydraulic structures, *J. Hydraulic. Eng., ASCE,* Vol.131. No.12, 2005, pp.1074-1087.
- [5] **Yeo, H. K., Kang, J. G., Kim, S. J.** An Experimental Study on Downstream Recirculation Zone of Single Groyne Condition, XXXI IAHR Congress, Korea, 2005, pp. 5101-5110.
- [6] **Karami H.** Experimental study of the effects of a side groyne length and interval on the scour pattern around the main groyne. M.SC thesis, Amirkabir University of technology, 2006.
- [7] **Xuelin, T., Xiang, D. and Zhicong, C.** Large eddy simulations of three-dimensional flows around a spur dike, *Journal for Tsinghua Science and Technology,* Vol 11, No. 1, 2006, pp.117-123.
- [8] **Yossef M. F.M. and Rupperecht R.** Modeling the flow and morphology in groyne fields, *River flow 2006,* Taylor and Francis Group, 2006, pp.1707.
- [9] **Ghodsian M., Vaghefi M., and Panahpour N.,** Experimental investigation of the separation zone around a groyne in the 90 degree bend, *4th National congress in civil engineering,* 2007.
- [10] **Keshavarz M.H., Hakim-Rad H.** Numerical Simulation of Flow Pattern around the Perpendicular and Inclined Groynes using Finite volume method, *7th International Conferences on Coasts, Ports and Marine Structures,* 2007.
- [11] **Ho J., Yeo H.K., Coonrod J., and Ahn W.** Numerical modeling study for flow pattern changes Induced by single groyne; congress, 32nd international association of hydraulic engineering and research, harmonizing the demands of art and nature in hydraulics Corila , Venice, 2007.
- [12] **Minor B., Rennie C.D., Townsend R.D.;** "Barbs" for river bend bank protection: application of a three-dimensional numerical model, *Canadian Journal of Civil Engineering,* Vol. 34, No. 9, 2007, pp. 1087-1095.
- [13] **Teraguchi H., Nakagawa H. and Zhang H.** Study on Flow and Bed Deformation around Impermeable and Permeable Groins, *8th ICHE, Nagoya, 8-12 September 2008,* pp. 367-370.
- [14] **Kang J., Yeo H., Kim S.,** Experimental Study on the Flow Characteristics around the Refraction groyne, *Vol.3, No.8, 2011,* pp.842-850.
- [15] **Shahrokhii M. and Sarveram H.** Three-dimensional simulation of flow around a groyne with large-eddy turbulence model, *Journal of Food, Agriculture & Environment,* Vol. 9, No. 3&4, 2011, pp.677-681.
- [16] **Sharma, K. and Mohapatra, P.** Separation Zone in Flow past a Spur Dyke on Rigid Bed Meandering Channel, *J. Hydraul. Eng.,* Vol. 138, No. 10, 2012, pp. 897-901.
- [17] **Punmia B. C. and Brij Basi Lal Pande;** *Irrigation and Water Power Engineering,* LAXMI publications, Delhi, 2005.
- [18] **Zhang H. and Nakagawa H.** Scour around Spur Dyke: Recent advances and Future researches, *Annals of Disas.Prev. Res. Inst., Kyoto Univ.,* No.51 B, 2008.
- [19] **Chen, F.Y. and Ikeda, S.** Horizontal separation flows in shallow open channels with spur dikes, *J. Hydrosic. & Hydraul. Eng., JSCE,* Vol. 15, No.2, 1997, pp. 15-30.
- [20] **FLUENT user's guide manual-version 6.3.26.** *Fluent Incor*